Biogeosciences Discuss., 5, 971–1015, 2008
www.biogeosciences-discuss.net/5/971/2008/
© Author(s) 2008. This work is distributed under
the Creative Commons Attribution 3.0 License.

Biogeosciences Discussions

Biogeosciences Discussions is the access reviewed discussion forum of *Biogeosciences*

Biogeochemical processes and microbial diversity of the Gullfaks and Tommeliten methane seeps (Northern North Sea)

G. Wegener[1], M. Shovitri[1], K. Knittel[1], H. Niemann[1,2,*], M. Hovland[3], and A. Boetius[1,2,4]

[1]Max Planck Institute for Marine Microbiology, Bremen, Germany
[2]Alfred Wegener Institute for Polar and Marine Research, Bremerhaven, Germany
[3]Statoil, Stavanger, Norway
[4]Jacobs University Bremen, Bremen, Germany
[*]present address: Institute for Environmental Geoscience, University of Basel, Switzerland

Received: 21 January 2008 – Accepted: 25 January 2008 – Published: 25 February 2008

Correspondence to: G. Wegener (gwegener@mpi-bremen.de)

Published by Copernicus Publications on behalf of the European Geosciences Union.

Abstract

Fluid-flow related seafloor structures and gas seeps were detected in the North Sea in the 1970s and 1980s by acoustic sub-bottom profiling and oil rig surveys. A variety of features like pockmarks, gas vents and authigenic carbonate cements were found to be associated with sites of oil and gas exploration, indicating a link between these surface structures and underlying deep hydrocarbon reservoirs. In this study we performed acoustic surveys and videographic observation at Gullfaks, Holene Trench, Tommeliten, Witch's Hole and the giant pockmarks of the UK Block 15/25, to investigate the occurrence and distribution of cold seep ecosystems in the Northern North Sea. The most active gas seep sites, i.e. Gullfaks and Tommeliten, were investigated in detail: at both sites gas bubbles escaped continuously from small holes in the seabed to the water column, reaching the upper mixed surface layer as indicated by acoustic images of the gas flares. At Gullfaks a 0.1 km^2 large gas emission site was detected on a flat sandy seabed, covered by filamentous sulfide-oxidizing bacteria. At Tommeliten we found a patchy distribution of small bacterial mats indicating sites of gas seepage. Here the seafloor consists of layers of sand and stiff clay, and gas emission was observed from small cracks in the seafloor. At both sites the anaerobic oxidation of methane (AOM) coupled to sulfate reduction is the major source of sulfide. Molecular analyses targeting specific lipid biomarkers and 16 S rRNA gene sequences identified an active microbial community dominated by sulfide-oxidizing and sulfate-reducing bacteria (SRB) as well as methanotrophic bacteria and archaea. Carbon isotope values of specific microbial fatty acids and alcohols were highly depleted, indicating that the microbial community at both gas seeps incorporates methane or its metabolites. The microbial community composition of both shallow seeps show high similarities to the deep water seeps associated with gas hydrates such as Hydrate Ridge or Eel River basin.

BGD

5, 971–1015, 2008

1 Introduction

The North Sea is a marginal sea of the Atlantic on the European continental shelf. Its sedimentary basin, especially the Western and Northern areas, hosts large gas and oil fields which are exploited since the 1970s. Leaking methane reservoirs are a major source for shallow gas accumulations and emission into the water column and atmosphere (Hovland and Judd, 1988; Rehder et al., 1998; Judd and Hovland 2007). In the North Sea, eruptive gas ebullition through impermeable seabed consisting of stiff glacial clays leads to the formation of small craters at the seafloor, also known as pockmarks (Hovland and Judd, 1988). These pockmarks have diameters in the range of few to several hundred meters and are widespread in gas and oil fields of the central and northern North Sea. Intensive bathymetric and videographic surveys by the British Geological Survey and oil industry have led to a good understanding of the distribution of these and other gas escape structures in the North Sea (Judd and Hovland, 2007). As part of the 5th EU framework project METROL "Methane fluxes in ocean margin sediments: microbiological and geochemical control" we have studied the distribution, biogeochemistry and microbiology of gas seepage in the North Sea, to identify potential sites of methane emission to the atmosphere, and to better understand the functioning of the associated shallow water seep ecosystems.

Although methane is abundant in the seafloor, the oceans account for only 3 to 5% of the global atmospheric methane flux (Reeburgh, 2007). Aerobic and anaerobic microbial methane consumption almost completely control the gas flux into the water column and atmosphere, except at sites of high fluid flow and free gas ebullition (Valentine and Reeburgh, 2000). The anaerobic oxidation of methane with sulfate as terminal electron acceptor is the dominant biogeochemical process in gassy sediments (Hinrichs and Boetius, 2002). Its net reaction can be described according to Eq. (1), but the underlying biochemistry of this process remains unknown (Widdel et al., 2007).

$$CH_4 + SO_4^{2-} \longrightarrow HCO_3^- + HS^- + H_2O \qquad \text{(R1)}$$

Several phylogenetic clades of archaea related to the order *Methanosarcinales* were

identified as anaerobic methanotrophs by analyses of 16 S rRNA gene sequences and of stable isotope signatures of specific biomarkers (Hinrichs et al., 1999; Boetius et al., 2000; Orphan et al., 2001b; Niemann et al., 2006). In most seep habitats archaea form consortia with sulfate-reducing bacteria of the *Desulfosarcina/Desulfococcus* or *Desulfobulbus* groups (Knittel et al., 2003; Niemann et al., 2006; Lösekann et al., 2007). These associations are commonly attributed to obligate syntrophy, in which the archaeal partner activates and metabolizes methane, providing an intermediate that is scavenged by the sulfate-reducing partner (Nauhaus et al., 2002; 2007). Analyses of carbon isotopes in seep ecosystems have shown a tight link between methane, the microbial consortia, authigenic carbonate precipitates and higher trophic levels in the food web (Hovland et al., 1985; Ritger et al., 1987; Hinrichs and Boetius, 2002; Hovland et al., 2002; Levin, 2005). Deep water gas seeps often support an enormous biomass of free-living and symbiotic microbial life that is nourished by the oxidation of methane and the product of its anaerobic oxidation, sulfide. A prominent feature of such seeps are mat-forming chemoautotrophic bacteria using sulfide as energy source, including *Beggiatoa* (Treude et al., 2003; Joye et al., 2004), and *Arcobacter* (Omoregie et al.[1]). Furthermore, authigenic carbonates related to anaerobic oxidation of methane (AOM) are found at many seeps. The precipitation of these carbonates is possibly related to an increase of pore water alkalinity due to AOM (Luff and Wallmann, 2003). Carbonate outcrops attract a variety of hardground fauna like corals, ophiurids, sponges and bivalves (Hovland and Risk, 2003; Niemann et al., 2005). Ultimately, the carbonate precipitation associated with AOM can fill and seal gas escape conduits (Hovland, 2002).

Biogeochemical research efforts on cold seeps during the last decade mainly focused on deep water systems, especially those associated with gas hydrates. As a consequence, much more is known about these systems than about shallow water seeps in estuaries and shelf seas, despite their potential relevance for gas emission

[1]Omoregie, E., Niemann, H., Masterlerz, V., de Lange, G., Stadnitskaia, A., Foucher, J.-P., and Boetius, A.: Anaerobic oxidation of methane and sulfate, Mar. Geol., in review, 2008.

to the atmosphere. Specifically in the Northern North Sea, where the water column is frequently mixed by storms, methane emission from the seabed is likely to result in an export of this greenhouse gas to the atmosphere. However, well constrained estimates of the methane flux from the seabed to the atmosphere are still missing for the North Sea.

Here we investigated several pockmarks and potential sites of gas seepage of the Northern North Sea. Sediments were sampled from sulfide oxidizing bacterial mats which were associated with gas ebullition. Based on the concentration and carbon isotopy of specific lipid biomarkers, as well as by 16 S rRNA sequence analysis, we describe the microbial communities of the two active shallow water seeps in the North Sea (Gullfaks and Tommeliten). Furthermore, their phylogenetic and biogeochemical characteristics are compared with those of known deep water cold seep communities to investigate whether shallow and deep seeps are populated by different types of methanotrophs.

2 Material and methods

2.1 Sampling sites

Figure 1 gives an overview on the cold seep sites in the North Sea visited during the METROL cruises (R/V Heincke cruises HE169, HE180, HE208 and R/V Alkor cruise AL267; also see Table 1). For all investigated sites detailed background information was obtained previously during extensive geological surveys including seismic and sonar monitoring of seabed and water column features, as well as by videographic exploration using towed cameras and ROVs (Hovland and Judd, 1988). Gas emissions at Tommeliten and Gullfaks have been documented for a period over 25 years (Niemann et al., 2005; Judd and Hovland, 2007).

Gullfaks is one of the four major Norwegian oil and gas fields, located in the north-eastern edge of the North Sea Plateau. The water depth in this area is ca. 140 m

CC BY

and deepens northeastwards towards the Norwegian trench (Hovland, 2007). During the last glacial maximum the plateau was exposed and coastal sands were deposited. Younger sediments of the Holocene have not been found in this area because tidal currents prevent deposition (Eisma and Kalf, 1987). The Gullfaks hydrocarbon reservoir is situated in a depth of nearly 3 km (Hovland and Judd, 1988). Shallow gas accumulations formed above the leaky reservoir at depths between 300 and 450 m below the seafloor (m.b.s.f.) (Judd and Hovland, 2007).

Tommeliten lies in the greater Ekofisk area north of the central North Sea (Hovland and Judd, 1988; Hovland, 2002; Judd and Hovland, 2007) at a water depth of 75 m. This gas field is associated with salt diapirs at about 1 km bsf, and has already been fully exploited (Hovland, 2002). Seismic profiles indicate extensive gas escape pathways in the seabed above the deposit. Eruptive discharge of free gas probably formed the shallow pockmarks which lie 0.5–1 m below the surrounding seabed level (Hovland and Sommerville, 1985). The sediments consist of sands, silt and marl (Niemann et al., 2005). Associated with gas leakage pathways are calcareous cements, some of which extend above the seafloor and form reefs populated by diverse anthozoa and other hardground fauna (Hovland and Judd, 1988; Niemann et al., 2005). Acoustic turbidity indicated the presence of free gas in the seabed in an area of about 0.12 km^2. Sonar surveys revealed gas escape to the water column, and accordingly, numerous gas seeps associated with whitish bacterial mats were observed during ROV surveys (Hovland et al. 1993; Judd and Hovland, 2007; Niemann et al., 2005). Gas seepage was confined to about 120 individual bubble streams in an area of 6500 m^2. An emission of 47 g $CH_4 m^{-2}$ was estimated for this seepage area (Hovland et al., 1993). In the vicinity of the gas vents, elevated methane concentrations and gas bubbles were found in the seabed, at a sediment depth of 1–5 m.b.s.f., associated with layers of carbonate precipitates and cements (Niemann et al., 2005). These observations and biogeochemical rate measurements indicate that most methane may be consumed in the seafloor, but that considerable gas escape to the water column occurs through cracks and fissures (Niemann et al., 2005). The carbon isotope signature of methane

CC BY

emitted from the seafloor of −45.6‰ indicates its thermogenic origin (Hovland and Sommerville, 1985; Hovland and Judd, 1988).

3 Seafloor observations

During the cruises HE169, HE180, HE208 and AL267 (Table 1), several seep locations of the North Sea were visited (Fig. 1). Gas flares were detected using the sediment echo sounder system SES-2000 provided by INNOMAR (Rostock, Germany). The emitter induces two primary frequencies near 100 kHz to generate secondary bandwidths of 4 and 15 kHz. The long waves were used to visualize shallow sea floor structures and layering. Water depth and gas flares were recorded with the 15 kHz spectrum, while sediment features were observed with a 4 kHz spectrum. Several acoustic transects were evaluated to quantify the gas flares and their extensions, and to localize the flare source at the seafloor. Video observations were performed with the ROV Sprint (Alfred Wegener Institute for Polar and Marine Research, Bremerhaven; HE169), the towed camera system of the AWI (HE180) or the MPI (Spy, Mariscope, Kiel; HE208), or via a remotely operating vehicle at Tommeliten (ROV Cherokee, MARUM, Bremen; AL267).

4 Sediment sampling

At Gullfaks sediments were sampled in May 2004 (HE208) using a video-guided multiple corer system (MUC; Octopus, Kiel). The samples were recovered from an area densely covered with bacterial mats where gas ebullition was observed. The coarse sands limited MUC penetration depth to max 30 cm. The highly permeable sands did not allow vertical subsampling of the MUCs at high resolution, because porewater was lost during subsampling.

The gas flare mapping and videographic observation at Tommeliten indicated an area of gas emission, which consisted of a few small patches of bacterial mats with

diameters <50 centimeters, spaced apart by 10–100 m, from most of which a single stream of gas bubbles emerged. Sampling of these patchy gas vents was only possible with the ROV Cherokee to which we mounted 3×3.8 cm diameter push cores. The cores were sampled in 3 cm intervals.

Sediment porosity, sulfate and methane concentrations were determined following the METROL protocol (http://www.metrol.org/index.php?bereich=1). In situ methane concentrations were calculated using PHREEQC, Version 2, US Geological Survey, 2007. Samples for molecular, microbiological and biomarker analyses were processed as described below.

Radiotracer based in vitro measurements of AOM and SR were performed in the home laboratory. Sediment samples stored anoxically in wide mouth bottles with artificial, anaerobic seawater medium (28 mM Sulfate, 30 mM carbonate, 1 mM sulfide, equilibrated at a pH of 7.2; see also Widdel and Bak, 1992) were transferred into Hungate tubes, refilled with medium and brought into equilibrium with one atmosphere of methane (Krüger et al., 2005). Controls without methane addition were prepared to determine methane independent SR. Rates were determined from replicate incubations (n≥3). After one day of equilibration, $^{35}SO_4$ (50 kBq dissolved in 10 μl water) for SR and $^{14}CH_4$ (10 kBq dissolved in 50 μl water) for AOM were injected into the Hungate tubes through a butyl rubber septum. Samples were incubated for 7 days at in situ temperatures (8°C). The reactions were stopped by transferring the samples into zinc acetate and NaOH solution, respectively (Treude et al., 2003). Further processing of AOM and SR samples was carried out as described previously (Treude et al., 2003; Kallmeyer et al., 2004), respectively. Concentrations and activities of the reactants (methane or sulfate) and the activities of the products (sulfide or carbonate) were measured to determine AOM and SR rates according to the following formulas:

$$\text{AOMrate} = \frac{[CH_4] \cdot a^{14\,C}\text{carbonate}}{t \cdot a^{14\,C}\text{methane}}, \quad (1)$$

$$\mathrm{SRR} = \frac{[\mathrm{SO_4}] \cdot \mathrm{aTRIS}}{t \cdot \mathrm{aTOT} \cdot m_{\mathrm{sed}}} \cdot 1.06, \quad (2)$$

In Eq. (2) (CH_4) is the concentration of methane, a^{14C}methane and a^{14C} carbonate the activity of the reactant and the product of AOM (Treude et al., 2003). In Eq. 3, (SO_4) is the concentration of sulfate, aTRIS the activity of the total reduced inorganic sulfur, aTOT is the total activity of sulfide and sulfate and t is the reaction time. The factor 1.06 accounts for the discrimination of the heavier radio nucleotide ^{35}S (Jørgensen and Fenchel, 1974).

Total organic carbon content (TOC) and carbon nitrogen ratios (C/N) were analyzed from freeze-dried samples. Briefly, inorganic carbon (carbonate) was removed via HCl acidification. Subsequently, 20 to 30 mg of homogenized samples were filled in zinc cartridges and organic carbon and nitrogen was measured in a CNS analyzer (Carlo Erba NA 1500 CNS analyzer).

4.1 Biomarker analyses

Lipid biomarker extraction from 10–17 g wet sediment was carried out as described in detail elsewhere (Elvert et al., 2003). Briefly, defined concentrations of cholestane, nonadecanol and nonadecanolic acid with known $\delta^{13}C$ values were added to the sediments prior to extraction as internal standards for hydrocarbons, alcohols and fatty acids, respectively. Total lipids were extracted from the sediment by ultrasonification with organic solvents of decreasing polarity. Esterified fatty acids were cleaved by saponification with methanolic KOH solution. From this mixture, the neutral fraction (mainly hydrocarbons and alcohols) was extracted with hexane. After subsequent acidification, fatty acids were extracted with hexane. For analysis, fatty acids were methylated using BF_3 in methanol yielding fatty acid methyl esters (FAMES).

The neutral fraction was further separated into hydrocarbons, ketones and alcohols on a SPE cartridge with solvents of increasing polarity (Niemann et al., 2005). The ketone fraction was not further analyzed. Shortly before analyses alcohols were methy-

CC BY

lated to trimethylsilyl (TMS) ethers using bis(trimethylsilyl)triflouracetamid (BSTFA). Concentration and identity of single lipid compounds was determined by gas chromatography (GC) and gas chromatography-mass spectrometry (GC-MS) analysis, respectively (Elvert et al., 2003, 2005; Niemann et al, 2005). Double bound positions of monoeonic fatty acids were determined analyzing their dimethyl disulfide (DMDS) adducts according to Moss and Labert-Faeir (1989). δ^{13}C-values of single lipid compounds were determined by GC-IRMS analyses according to Elvert et al. (2003). Concentration and isotopic signatures of fatty acid and alcohol were corrected for the additional carbon atoms added during derivatisation.

5 DNA extraction, PCR amplification and clone library construction

From both sites DNA was extracted from 2 g of wet sediment (1–3 cm depth) using bio101 soil kit (Bio101, La Jolla, California). Domain-specific primers were used to amplify almost full-length 16 S rRNA genes from the extracted chromosomal DNA by PCR. For Bacteria, primers GM3F (Muyzer et al., 1995) and EUB1492 (Kane et al., 1993) were used, for Archaea, the primers ARCH20F (Massana et al., 1997) and Uni1392 (Lane et al., 1985) were used. PCRs were performed (30 cycles) and products purified as described previously (Ravenschlag et al., 1999). DNA was ligated in the pGEM-T-Easy vector (Promega, Madison, WI) and transformed into E. coli TOP10 cells (Invitrogen, Carlsbad, CA) following manufacturer's recommendation.

5.1 Sequencing and phylogenetic analysis

Sequencing was performed by Taq cycle sequencing with a model ABI377 sequencer (Applied Biosystems). The presence of chimeric sequences in the clone libraries was determined with the CHIMERA_CHECK program of the Ribosomal Database Project II (Center for Microbial Ecology, Michigan State University, http://rdp8.cme.msu.edu/cgis/chimera.cgi?su=SSU). Sequence data were analyzed with the ARB software package

CC BY

(Ludwig et al., 2004). Phylogenetic trees were calculated with the ODP 204 sequences from this project together with reference sequences, which were available in the EMBL, GenBank and DDJB databases by maximum-likelihood and neighbor-joining analysis with different sets of filters.

5.2 Cell counts and CARD-FISH (Catalyzed reporter deposition – fluorescence in situ hybridization)

The fixation for total cell counts and CARD-FISH were performed on-board directly after sampling. For both methods 2 ml of the sediment were added to 9 ml of 2% formaldehyde artificial seawater solution, respectively. After fixation for two hours CARD-FISH samples were washed three times with 1xPBS (10 mM sodium phosphate solution, 130 mM NaCl, adjusted to a pH of 7.2 by titration with Na_2HPO_4 or NaH_2PO_4) and finally stored in 1:1 PBS:ethanol solution at −20°C until further processing. Samples for total cell counts were stored in formalin at 4∘C.

For the sandy samples the total cell count/CARD-FISH protocol were optimized to separate the sands particles from the cells. Cells were dislodged from sediment grains and brought into solution with the supernatant by sonicating each samples on ice for 2 min at 50 W. This procedure was repeated four times and supernatants were combined. Total cell numbers were determined from the supernatant using acridine orange direct counting (AODC; Meyer-Reil, 1983).

CARD-FISH was performed following the protocol of Pernthaler (2002). The sediment samples were brought to a final dilution of 1:2000 to 1:4000 and filtered onto 0.2 μm GTTP filters (Millipore, Eschbonn, Germany). The probes used in this study (all purchased from biomers.net GmbH, Ulm, Germany) were EUB 338 I-III specific for most Bacteria (Amann et al., 1990; Daims et al., 1999), DSS658 specific for Desulfosarcina spp., Desulfococcus spp. and closely related clone sequences (Manz et al., 1998), Arch915 specific for most Archaea (Stahl and Amann, 1991), and probes ANME1-350 (Boetius et al., 2000), ANME2a-647, ANME2c-622 (Knittel et al., 2005) and ANME3-1249 (Niemann et al., 2006) specific for ANME-1, -2a, -2c, and -3 archaeal

CC BY

cells, respectively. Cell permeabilization and probe hybridization were performed according to the author's instructions. For reference cell numbers, samples were also stained with 4′6′-diamidino-2-phenlyindole (DAPI) for 15 min (1 μg/ml) and washed with sterile filtered water and ethanol for 60 and 30 sec, respectively. Air-dried filters were imbedded in Citifluor (Citifluor Ltd., Leicester, UK). Cells were counted using an epifluorescence microscope (Axioplan, Zeiss, Germany). At least 1000 cells in randomly chosen fields were counted per sample. To quantify aggregates of ANME-2a, -2c and -3 up to 250 grids were counted under 400-fold magnification. Dual hybridizations for sulfate reducers (DSS) and archaea (ANME-2a and -2c) were performed using different fluorescence dyes (cy3 and cy5) and images were taken with a confocal laser scanning microscope (LSM510; Carl Zeiss, Jena, Germany).

6 Results and discussion

6.1 Distribution of active seeps in the Northern North Sea

The presence of gas flares indicating active methane seepage from the seabed was detected at different fluid flow-related seafloor structures visited during the METROL cruises. Large and abundant gas flares were found at Tommeliten, Gullfaks, Snow White's Hole and the giant pockmarks of UK block 15/25 (Figs. 1, 2; Table 1).

The pockmarks of UK Block 15/25, Snow White's Hole and Witch's Hole are part of the Witch Ground formation, northwest of the Tommeliten seep area (Fig. 1, Hovland and Judd, 1988). During our cruises (HE180 and HE208), most of the 5 giant (Scanner, Scotia and Challenger formation) and two medium sized pockmarks of the UK Block 15/25 showed active seepage of methane from the deepest part of each depression (up to 17 m below the surrounding seafloor; Fig. 2c). Hovland et al. (1993) estimated the average flux at this location with 26 g $CH_4\,m^{-2}\,yr^{-1}$. In the center of the pockmarks we also observed carbonate outcrops which were populated with benthic organisms, mostly sea anemones. Unfortunately we were not able to sample the

CC BY

surface and subsurface cements at the bottom of the steep pockmarks because the gravity corer and multiple corer could not penetrate. The methane venting and the carbonate cements have been observed previously (Hovland and Judd, 1988) and during all expeditions to this site, indicating that the UK 15/25 pockmarks may have been continuously emitting methane to the hydrosphere for at least 2 decades. The gas flares at the UK 15/25 pockmarks reached up to 80 m below the sea surface. In contrast to earlier observations (Hovland and Judd, 1998), the Witch's Hole structure itself was presently dormant, but we found an active pockmark southwest of it, which we named Snow White's Hole (Fig. 2d). This structure emits a large gas flare extending about 80 m from the seafloor. However sampling directly at the flare was not possible most likely because of the presence of carbonate cements. Sampling in the vicinity of the gas flare at the edge of the pockmark recovered only oxidized non-seep sediments.

The Holene Trench is an open channel of ca. 1 km width located on the Norwegian Plateau in about 120 m water depth. Previous surveys showed an acoustic turbidity in the top most 30 m of the surface sediments indicating gas charged sediments (Hovland and Judd, 1988). During our survey, two places were found where the turbidity extends to the surface of the sea floor, which could be related to active seep sites. However, during HE-169 we could not find any traces for active seepage (Fig. 2b) and only beige, oxidized clay sediments were recovered by multiple corer sampling. The western slope of the Norwegian Trench hosts several pockmark-like structures, which do not show carbonate outcrops (Hovland and Judd, 1988). Our survey during cruise HE-169 did not reveal any traces of seepage and one grab sample recovered beige, oxidized sandy-silty sediments. Previous surveys in the Skagerrak found several pockmarks with active gas escapes and seepage related fauna (Dando et al., 1994; Rise et al., 1999). During HE-208 we did not observe gas seepage from the positions reported in Dando et al. 1994 (Fig. 2f).

For further investigations of the biogeochemistry and microbiology of shallow water cold seeps in the North Sea we focused on the Tommeliten and Gullfaks sites. The results from subsurface sampling of the Tommeliten seeps with help of a vibrocorer were

CC BY

already reported in Niemann et al. (2005). Here we focused on the hot spots for microbial methane turnover and methane emission which were associated with bacterial mats at both sites.

7 Gullfaks

7.1 Seafloor observations

The Gullfaks field is located on the North Sea Plateau (~150 m water depth) and on an ancient beach (140–190 m), respectively. The submerged beach was formed during the sea-level low of the last glacial maximum (Hovland and Judd, 1988). Pockmark-like depressions were absent, which may be explained by the sediment properties of this area. Pockmark formation is believed to be limited to silty or clayish seafloor with low permeability and may not occur in highly permeable sandy seafloors (Hovland and Judd, 1988; Judd, 2003). The flat seafloor of the Gullfaks seep area is composed of coarse sand and gravel. However, ripple structures observed during the ROV dives indicate episodically high bottom water current velocities. Several gas flares were found within an area of about 0.5 km^2, which was named "Heincke seep area" (Hovland, 2007). The flares extended up to 120 meters above the seafloor, reaching the mixed water layer (Fig. 2a). Visual observations of the seafloor showed 1–2 bubble streams escaping from the sands every 5 m^2 within a smaller area of 0.1 km^2 covered by microbial mats (Fig. 3a). The macroscopic appearance resembled mats formed by giant filamentous sulfide oxidizing bacteria, such as *Beggiatoa*, which establish above zones of high sulfide flux (Nelson et al., 1986). No megafauna was observed to populate the seep site or to graze upon the bacterial mats, but many large cod-like fish were observed in this area. Considering the solubility of methane in situ at a water depth of 150 m (equivalent to ~16 bar modeled with PREEQC, USGS), methane concentrations in the seabed should exceed 26 mM.

Multicorer sampling was conducted at Gullfaks in the bacterial mat field (Fig. 3a).

CC BY

Upon recovery, the sediment cores degassed strongly, releasing streams of methane bubbles into the overlaying water. The sediments smelled strongly of sulfide. The top 30 cm of sediment retrieved by multiple coring was unsorted, coarse to medium grained sands. Sediment porosity was on average 33%. Only the top surface layer of 1 to 5 cm was of beige color mixed with black particles, probably marking the oxygen penetration depth. The color shift to blackish sediments below indicated the change of redox conditions to negative values and the presence of free sulfide and iron sulfide precipitations. Within the gassy sediment abundant ferromagnetic minerals, probably magnetite or greigite, were found, indicating a connection of methane and iron fluxes. Total organic carbon showed average values of only 0.17%, indicating that the main source for the observed high sulfide concentrations may be methane rather than deposited organic material.

7.2 Microbial methane oxidation and sulfate reduction

From all six multicorer samples retrieved from the mat covered area, methane oxidation and sulfate reduction rate measurements were performed using replicate subsamples of the bulk sediments from the top 25 cm. Methane oxidation rates ranged from 0.006 μmol g^{-1} to 0.18 μmol g^{-1} dry weight d^{-1} and sulfate reduction rates (SRR) from 0.05 μmol g^{-1} to 0.3 μmol g^{-1} dry sediment d^{-1}. In control measurements without methane, SRR was negligible, indicating that methane was the dominant electron donor for sulfate reduction. The integrated methane oxidation rates averaged 12.5 mmol m^{-2} d^{-1} and the integrated SRR 18.5 mmol m^{-2} d^{-1}. These are comparatively high rates which fall within the range of other measurements from bacterial mat covered seep sites like Hydrate Ridge (5.1 to 99 mmol m^{-2} d^{-1}; (Treude et al., 2003) or Haakon Mosby Mud Volcano (4.5 mmol m^{-2} d^{-1}; Niemann et al., 2006). Using the mean methane oxidation rate from our incubations, a methane consumption of 15 t yr^{-1} can be roughly calculated for an area of 0.1 km^2. Based on quantifications of single gas bubble streams (Hovland et al., 1993) we estimated a gas flux to the water column of 76 t yr^{-1} for this area, which means that the microbial filter could consume at least 16%

CC BY

of the total gas flux. Of course, these are only rough estimates, as the gas streams may vary strongly in intensity and methane content.

7.3 Biomarker and carbon isotope signatures

The ^{13}C carbon signatures of methane at Gullfaks cover a range from −44.4‰ vs. PDB (Pee Dee Belemnite) at reservoir level (2,890 m below seafloor) to −70‰ at seafloor level (Judd and Hovland, 2007). The abundance of specific biomarker lipids and their stable carbon isotope signatures were analyzed to reveal the distribution of chemoautotrophic and methanotrophic microbial communities. The lipid concentrations and isotopic signatures of the Gullfaks microbial communities (Core 766) are shown in Table 2. In comparison to highly active seep sites such as Hydrate Ridge, concentrations of lipid biomarkers at Gullfaks and Tommeliten were low.

In surface sediments of Gullfaks monoeonic fatty acids were strongly dominant. Although these fatty acids are produced by a wide range of gram negative bacteria (Fang et al., 2005), their relative abundance can be used to trace specific microbial groups. The measured ratio for $C_{16:1\omega7c}$, $C_{18:1\omega7c}$ and $C_{16:0}$ of 68:18:14 was close to the ratio of 73:18:9 previously reported for *Beggiatoa* filaments covering cold seep sediments of the Gulf of Mexico (Zhang et al., 2005). The $\delta^{13}C$ values of the FA $C_{16:1\omega7c}$ and $C_{18:1\omega7c}$ (−41 and −57‰, respectively) extracted from the bacteria covered sands, indicate a substantial contribution of autotrophic carbon fixation as previously found for several species of giant filamentous sulfide oxidizers (Nelson and Jannasch, 1983; Nelson et al., 1986; Nelson et al., 1989). In addition to signatures of sulfide oxidizing bacteria, substantial amount of diplopterol were found. This hopanoid is synthesized by several aerobic bacteria including methanotrophs (Rohmer et al., 1984). A methanotrophic origin of this biomarker at Gullfaks is likely because of its highly depleted stable carbon composition (−84%).

Characteristic lipids for seep associated sulfate reducing proteobacteria are $C_{16:1\omega5c}$, cy-$C_{17:0\omega5,6}$, (Blumenberg et al., 2004; Elvert et al., 2003; Niemann et al., 2005; Niemann and Elvert, in press). We found a biomarker pattern with a clear dominance of

CC BY

$C_{16:1\omega5c}$ relative to $iC_{15:0}$ previously identified as a typical signature for populations of sulfate reducers associated to ANME-2 and -3 dominated communities (Niemann and Elvert, in press). Specifically the $\delta^{13}C$ value of $C_{16:1\omega5c}$, of −82‰ strongly indicates an incorporation of methane-derived carbon. Previously, Niemann et al. (2006) reported an association of *Desulfobulbus* related bacteria to ANME-3. We did not find the typical biomarker $C_{17:1\omega6}$ of this group, nor the related sequences in the Gullfaks sediments (Lösekann et al., 2007). Instead, substantial amounts of the ^{13}C depleted FA cy-$C_{17:0\omega5,6}$ (−97‰) provides evidence for a dominance of SRB of the Seep-SRB1 cluster associated with ANME-2 (Elvert et al., 2003; Niemann et al., 2006; Niemann and Elvert, in press). The fatty acids iso- and anteiso-$C_{15:0}$ were less depleted with signatures of −41 to −52‰. From the difference in the isotope signatures of these two groups of sulfate reducing bacteria, it appears likely that a diverse community of sulfate reducers is present in the Gullfaks sediments, of which only some are coupled to the anaerobic methanotrophs.

Several clades of ANME produce ^{13}C-depleted archaeol and sn2-hydroxyarchaeol which are used as biomarkers for AOM (Orphan et al., 2001a; Michaelis et al., 2002; Blumenberg et al., 2004). At Gullfaks, sn2-hydroxyarchaeol was 2.2–2.9 fold more abundant than archaeol, indicating the dominance of ANME-2 populations (Blumenberg et al., 2004; Niemann and Elvert, in press). Both compounds were highly depleted in ^{13}C, with $\delta^{13}C$-values of −11‰ and −117‰. Assuming that methane was the sole carbon source ($\delta^{13}C$-methane=−70 (Judd and Hovland, 2007) for the synthesis of archaeol and sn2-hydroxyarchaeol, this is equivalent to a ^{13}C fractionation factor of −45 to −47‰. This is in the range of isotope fractionation factors previously reported for anaerobic methanotrophic archaea from different marine settings (Hinrichs and Boetius, 2002; Niemann and Elvert, in press).

Microbial diversity and community composition based on 16S rRNA gene analyses. The bacterial 16S rRNA gene library from the gassy sands at Gullfaks comprised 69 gene sequences and was clearly dominated by microorganisms associated with seep ecosystems. We found different groups of sulfate-reducing bacteria and thiotrophic

CC BY

as well as methylotrophic bacteria (Table 3, Fig. 4). 15 sequences belonged to relatives of sulfur-oxidizing symbiotic *Gammaproteobacteria* usually hosted by different marine worms or mussels. No closely related sequences of filamentous sulfide oxidizers were found, although these were visually present in the sample from which DNA was extracted. Sequences related to methylotrophic bacteria (*Methylomonas* and *Methylophaga* relatives) were also abundant (6 sequences) matching our results from the biomarker studies. We found 10 sequences of *Deltaproteobacteria*, which were all related to SRB of the *Desulfosarcina/Desulfococcus* group (Seep-SRB-1), which is the partner of ANME-1 and -2 (Knittel et al., 2003). 19 clones were related to the cluster of *Cytophaga – Flavobacterium – Bacteriodetes* (CFB) which is a diverse group of bacteria commonly found in the plankton and sediment involved in the degradation of complex organic matter, but which also occur at cold seep ecosystems (Knittel et al., 2003).

The archaeal 16 S rRNA sequence library was strongly dominated by *Euryarchaeota* sequences. Sixty three of 69 analyzed clones were affiliated with ANME-2a (Table 3, Fig. 5), the most common group of anaerobic methane oxidizers in gas hydrate bearing environments (Knittel et al., 2005). The ANME-2a clones were highly similar to sequences from other seep sites (Fig. 5), e.g. the Santa Barbara Basin (Orphan et al., 2001a), Hydrate Ridge (Knittel et al., 2005), the Gulf of Mexico seeps (Mills et al., 2003), and a Pacific carbon dioxide seep (Inagaki et al., 2006). Sequences related to other groups performing AOM, such as ANME-1, -2c, -3, were not found in our library. The only other euryarchaeotal sequence belonged to the Marine Benthic Group D. Five clones belonged to the phylum *Crenarchaeota* including three clones of the Marine Benthic Group B which is regularly found at seeps (Knittel et al., 2005). The biogeochemical function of members of both archaeal marine benthic groups has not been identified yet. A study based on isotopic signatures of lipid biomarkers suggests that subsurface *Crenarchaeota* of the Marine Benthic Group B could be heterotrophic, although they are commonly associated with methane sulfate transition zones (Biddle et al., 2006).

CC BY

Total cell numbers in surface sediments at Gullfaks were quite high with 6.7×10^9 and 7.9×10^9 single cells ml^{-1} sediment in the uppermost 10 cm at station 771 and 766, respectively (Table 4). These cell numbers are higher than previously reported for non-seep sandy sediments (Llobet-Brossa et al., 1998; Wieringa et al., 2000; Rusch et al., 2001, 2003) and underline the stimulating effect of methane seepage on the microbial community inhabiting sands. The only other published cell counts from methane percolated sands showed numbers similar to those found at Gullfaks (Ishii et al., 2004). At a depth of 20–30 cm cell numbers decreased considerably to 0.85×10^9 and 1.3×10^9 cells ml^{-1}, indicating that the peak of microbial activity is in the upper 10 cm. The ratio of bacterial and archaeal cells were quantified by CARD-FISH. *Bacteria* comprised 29–50% and Archaea 8–16% of the DAPI stained cells. We found relatively high numbers of ANME 2a- and ANME 2c- cell aggregates; however, they did not reach the size and abundance of deep sea sites such as Hydrate Ridge (Nauhaus et al., 2002, 2007; Knittel et al., 2005). ANME-2a cells were clustering in dense, typically spherical aggregates associated with sulfate reducing bacteria in diameters of up to 10 μm (Fig. 6). ANME-2c cells were detected in less dense, small aggregates. The highest counts of ANME aggregates (8.4×10^6 ANME-2c aggregates at station 766, 6.6×10^6 ANME-2a-aggregates at 771) and ANME single cells (1.6×10^8 cells ml^{-1}) were also found in the top 10 cm, matching the distribution of total cell numbers. The abundance of methanotrophic microorganisms strongly decreased with depth, providing evidence for a near surface peak of AOM activity. This may indicate that the highest availability of both methane and sulfate as main energy source is generally found in the surface sediment horizon. Interestingly, this horizon is likely to experience temporary flushing with oxygenated bottom waters, as indicated by the observed ripple structures on the seafloor, which are presumably caused by high bottom water currents. This should have a negative effect on the anaerobic microbial communities. However, it is possible that the high upward advection of gas may restrict the downward diffusion of oxygenated bottom waters at the seep site.

The Gullfaks seep is the first site at which abundant single cells of ANME-2a and

ANME-2c were detected. Previously, only ANME-1 (Orphan et al., 2002; Niemann et al., 2005) and ANME-3 (Lösekann et al., 2007) were found as single cells. Monospecific ANME-2a or ANME-2c aggregates have been previously reported from Eckernförder Bay (Treude et al, 2005) and Eel River Basin (Orphan et al., 2002). ANME-2 cells aggregates without bacterial partner were also found to dominate specific regions of a microbial mat from the Black Sea (Treude et al., 2007).

8 Tommeliten seeps

8.1 Seafloor observations

The Tommeliten seep site lies at 75 m water depth and is part of the greater Ekofisk area of the Norwegian Block 1/9. In this area, the sedimentary rocks host a now exploited hydrocarbon reservoir. This reservoir is pierced by a salt diapir at about 1 km depth below the sea floor, and disturbances on seismic profiles indicate that free gas migrates to the sea floor (Hovland and Judd, 1988; Hovland, 2002).

Within an area of 0.5 km^2 at the Tommeliten site we observed several gas flares, which extended from the seafloor to the sea surface (Fig. 2f). Many of these flares were concentrated in a small area of about 0.06 km^2, which we assume to be the centre of the subsurface gas escape pathway. The distribution of the gas flares in 2005 (AL 267) was similar to the observations made in 2002 (HE180; Niemann et al., 2005). Previous expeditions to the Tommeliten seepage area used remotely operated vehicles (ROVs) for bottom observations and sampling, and documented streams of single methane bubbles of thermogenic origin ($\delta^{13}C$ −45.6‰), small patches of microbial mats and methane derived authigenic carbonates outcropping at the sea floor (Hovland and Sommerville, 1985; Hovland and Judd, 1988; Trasher et al., 1996; Niemann et al., 2005). Our observations by ROV in 2005 confirmed that most gas flares originated from small holes (1–5 cm diameter) in the seafloor emitting single streams of bubbles. They were associated with small patches of bacterial mats (30–50 cm in

CC BY

diameter, Fig. 3b). We sampled three cores from such bacterial mats. The recovered sediments below the mats were highly gassy and consisted of fine sands. In contrast, sediments a few meters away from the gas flares consisted of consolidated, hardly permeable marls enclosing layers of unsorted silt and sands above carbonate cements (Niemann et al., 2005). Accordingly, gas migration from the subsurface to the seabed may be limited to sandy horizons between the impermeable clays, and the gas bubbling may further erode the fine grain fraction. Upon recovery, the cores from these sediments continued to release methane gas as verified by GC measurements. This indicates a high in situ gas pressure in the seabed. At a water depth of 75 m the equilibrium methane concentrations in the interstitial waters in the direct vicinity of the gas ebullition sites could be around 12 mM.

8.2 Methane and sulfate turnover

The sample from a black patch from which gas escape was observed was composed of silty sediments, and contained little TOC of 0.22 to 0.32% w/w. Due to the small amount of sediment recovered, we could not measure AOM and SR rates. It can be assumed that the rates are locally very high due to the saturation with gas and the flux of sulfate from overlying bottom water into the bubble sites. However, for the subsurface sulfate methane transitions zones (SMTZ) associated with the gas-migration pathways at Tommeliten, Niemann et al. (2005) showed low AOM and SR rates of a few nmol $cm^{-3}\ d^{-1}$, resulting in ca 50 g $CH_4\ m^{-2}\ yr^{-1}$, or 0.3 t yr^{-1} for the whole seep area of ca. 6500 m^2. In comparison, the gas ebullition from the same site was estimated with 47 g $CH_4\ m^{-2}\ yr^{-1}$ (Hovland et al., 1993) suggesting a 50% efficiency of the microbial filter against methane. The higher methane consumption efficiency compared to Gullfaks could be due to the impermeable nature of the Tommeliten sediments allowing only for few gas leakage pathways.

CC BY

8.3 Biomarker and carbon isotope signatures

Similar to surface sediments at Gullfaks, monounsaturated fatty acids were also the dominant biomarker fraction in the surface sediments from the Tommeliten gas vents (Table 2). However, concentrations of these and other bacteria lipids were lower in comparison to the mat-covered sands at Gullfaks. The fatty acid distribution suggests the presence of sulfide oxidizing bacteria, but the ratio of $C_{16:1\omega7c}$ to $C_{18:1\omega7c}$ to $C_{16:0}$ (42:32:26) indicated a lower contribution to total bacterial biomass than in the Gullfaks sands.

In comparison to the Gullfaks seeps, the sediments from the Tommeliten gas vents contained similar amounts of archaeol but even more sn2-hydroxyarchaeol, indicating the dominance of ANME-2 populations. Both archaeol and sn2-hydroxyarchaeol were less depleted than at Gullfaks with $\delta^{13}C$ values of −86‰ and −90‰. However, considering the heavier isotopic signature of the source methane at Tommeliten ($\delta^{13}C$ CH_4 −46‰ Hovland 2002), a stable carbon isotope fractionation of the lipid biomass relative to source methane of more than 40‰ typical for AOM and comparable to that at Gullfaks was found.

The specific biomarkers for SRB associated with AOM such as $C_{16:1\omega5c}$, i-$C_{15:0}$, and cy-$C_{17:0}$ were similar in ratio but less abundant than at Gullfaks. The $\delta^{13}C$-values of $C_{16:1\omega5c}$ and cy-$C_{17:0}$ were relatively depleted with −51‰ and −59‰, respectively, whereas ai-$C_{15:0}$ showed substantially less depleted carbon isotope signatures of −34‰. Interestingly, the surface seep sediments at Tommeliten resembled the biomarker signatures in the authigenic carbonate outcrops, but differed substantially from subsurface sediments (Niemann et al., 2005). In the deep SMTZ Niemann et al. (2005) found a dominance of ANME-1 communities as indicated by the dominance of archaeol over hydroxyarchaeol and a typical fatty acid pattern typical for sulfate reducing partners of ANME-1 (Blumenberg et al. 2004; Niemann and Elvert, in press; Niemann et al., 2005). These results correlated with 16 S rRNA and FISH analyses (Niemann et al., 2005). We conclude that ANME-1 could be better adapted to the low

CC BY

energy conditions characteristic for deep sulfate methane transition zones, whereas ANME-2 dominates the advection driven highly active surface zones as already observed in some deep water seeps (Knittel et al., 2005).

8.4 Microbial diversity and community composition based on 16 S rRNA gene analyses

Similar to Gullfaks, the bacterial 16 S rRNA gene sequence library (Table 3) and the selected sequences in the phylogenetic tree (Fig. 4) obtained from sediments of Tommeliten showed a relatively high diversity of sulfate reducing bacteria including relatives of the uncultured Seep-SRB1 (ANME-2 partners), Seep-SRB2 (Eel2), and of *Desulfobacterium anilini*. Seep-SRB2 organisms have been retrieved from nearly all seep sediments (e.g. Knittel et al., 2003; Lösekann et al., 2007; Mills et al., 2005; Orphan et al., 2001b). However, their function remains unknown since no isolates are available. *Desulfobacterium anilini* relatives have been shown to oxidize different aromatic hydrocarbons such as naphthalene or xylene and could also have a function in hydrocarbon degradation at this site (for an overview see Widdel et al., 2007). Also a high number of clones related to *Desulfobulbus* were found. In cold seep sediments of the Haakon Mosby mud volcano (Barents Sea), the SRB community was dominated by such relatives of *Desulfobulbus,* which formed aggregates with anaerobic methanotrophs of the ANME-3 cluster (Niemann et al., 2006, Lösekann et al., 2007). Single ANME-3 cells and a few aggregates occurred in the Tommeliten cold seep sediments, but their abundance was too low to analyze the potential bacterial partners.

As predicted by the biomarker signatures, the archaeal gene sequence library of Tommeliten contained mainly relatives of ANME-1 and ANME-2c (Fig. 5). These were most closely related to sequences retrieved from gas hydrate bearing sediments such as the Eel River Basin, Hydrate Ridge, and the Gulf of Mexico. ANME-2a sequences were not represented in the clone library, although ANME-2a aggregates were detected by CARD-FISH (see below).

Cell counts in the cores 1274 K1 to K3 ranged from 4.1 to 5.8×10^9 cells ml^{-1} in

the top layer of sediment and hence were comparable to the cell numbers at Gullfaks. With depth, cell numbers decreased to 3.0×10^9 cell ml^{-1} (6–10 cm). Quantification with CARD-FISH indicated the presence of ANME-2a, ANME-2c and low numbers of ANME-3 single cells and aggregates. Sulfate reducing bacteria were highly abundant comprising up to one third of total single cells.

Hence, the microbial communities in gassy sediments below thiotrophic mats of both seep sites in the North Sea were dominated by anaerobic methanotrophs of the ANME-2 cluster, and their partner sulfate reducing bacteria. At Tommeliten, the AOM community in the mat covered surface sediments resembled more that of the Gullfaks seep and of the Tommeliten authigenic carbonates than that of the subsurface SMTZ community (Niemann et al., 2005). The microbial communities also comprised sequences from other microorganisms typically occurring in methane rich deep-water seep ecosystems such as the crenarchaeotal Marine Benthic Group B. Gene libraries and CARD-FISH counts indicated also differences between Gullfaks and Tommeliten AOM communities – such as the dominance of the ANME 2a cluster in Gullfaks cold seep sediments and the dominance of ANME 2c at Tommeliten, which may be a result of the different geological and hydrological features of both sites.

9 The North Sea seeps in comparison to deep water cold seeps

At the shallow water seeps of the Northern North Sea, methane emission from deep reservoirs has been observed for more than 20 years. The habitats investigated here are characterized by locally high advection of gaseous methane and ebullition of gas bubbles to the hydrosphere. Both Tommeliten and Gullfaks likely contribute to methane emission to the atmosphere as indicated by gas flares reaching to the upper mixed water layers. It would be an important future task to attempt quantification of gas emission to the atmosphere by monitoring flares and methane concentrations in the flares and the overlying surface waters.

In the interstitial porewaters of the Tommeliten and Gullfaks seeps, dissolved

CC BY

methane can reach concentrations of 12 mM and 25 mM, respectively. The highly permeable sands at Gullfaks allow the migration of gas bubbles through the sediment, leading to a relatively large seep area populated by methanotrophs and thiotrophs. The high upward advection of gas may restrict the downward diffusion of oxygenated bottom waters below a few cm, protecting the anaerobic methanotrophic communities, which showed very high activities in the top 10 cm. In contrast, the compact silty sands of Tommeliten allow gas migration only through small cracks in the seafloor sediments, restricting the distribution of methanotrophs and thiotrophs to small patches around the gas vents. Phylogenetic analysis of *Deltaproteobacteria* and *Euryarchaeota* at Gullfaks and Tommeliten indicate a high similarity of these to sequences from deep water seep sites, such as Hydrate Ridge (Boetius et al., 2000; Knittel et al., 2003; Knittel et al., 2005), Eel River Basin (Orphan et al., 2001b) or Guyamas Basin (Teske et al., 2002).

The concentrations of most of the AOM specific biomarker were about one order of magnitude lower at the investigated sites compared to deep water seep ecosystems such as Hydrate Ridge (Elvert et al., 2003) and Haakon Mosby Mud Volcano (Niemann et al., 2006). This finding was reflected in the low number of ANME aggregates of around 10^6 cm^{-3}. In deep water cold seeps such as Hydrate Ridge, Haakon Mosby and Eel River Basin, ANME aggregate numbers reach 10^8, comprising a large fraction of the total microbial biomass (>90%) (Knittel et al., 2005). A reason for this difference in ANME biomass could be the higher availability of dissolved methane in deep water seeps due to the increased solubility of methane at high hydrostatic pressures. Previous experiments indicate that AOM rates and the energy yield available for growth are higher at elevated methane concentrations (Nauhaus et al., 2002; 2007), which may support higher biomasses of AOM consortia. A second explanation for lower aggregate sizes in the North Sea may be the high bottom water currents causing relocation of particles, as well as sporadic oxygen influx into the sandy sediments. The only shallow water seeps known with higher biomass of ANME are the conspicuous methanotrophic microbial reefs of the Black Sea (Blumenberg et al., 2004; Treude et al., 2005). These lie in permanently anoxic waters and are hence protected from grazing.

BGD
5, 971–1015, 2008

10 Conclusions

Several gas seepages were mapped during the METROL cruises with R/V Heincke and Alkor. From these, we chose the two most active and accessible seepage areas, Tommeliten and Gullfaks, for detailed surveys using geochemical and molecular tools. At Gullfaks a seepage area of about 0.1 km^2 was characterized by a high density of gas vents and extensive coverage by thiotrophic bacterial mats. At Tommeliten gas vents were less dense and the bacterial mat covered areas were limited to small patches around small holes in the seafloor emitting gas. The different permeability of the seabed at both seep sites could explain the observed differences in the efficiency of the microbial filter against methane. From both sites considerable amounts of methane are emitted, some of which may reach the atmosphere as indicated by large gas flares reaching the upper mixed water layers. Specific biomarker and carbon isotope signatures, as well as 16 S rDNA gene sequences and fluorescence in situ hybridization of specific microbial groups indicated that the bacterial mat covered sediments were populated by active communities of ANME-2 and their sulfate reducing partner bacteria. Archaeal biomarkers were about 40‰ to 50‰ depleted in ^{13}C relative to the carbon source methane. Specific fatty acids of sulfate reducers involved in AOM were also considerably depleted in ^{13}C indicating that they partially assimilate methane derived carbon. The 16 S rRNA based gene libraries of both sites mostly included sequences from known groups of deep water cold seep microorganisms, indicating that water depth or other oceanographic conditions may not be limiting the dispersal of these groups. In contrast, distinct differences were found between the microbial community in the mat covered surface sediments (dominated by ANME-2) to those of the subsurface sulfate methane transition zone at Tommeliten (dominated by ANME-1), suggesting that different energy availabilities may select for different methanotrophic communities.

Acknowledgements. This study was conducted as part of the METROL project (http://www.metrol.org) of the 5th framework program of the European Commission (EVK-3-CT-2002-

00080). We thank captain, crew and shipboard scientists of R/V Heincke cruise HE-169 HE-180 and HE-208 and R/V Alkor cruise AL-267 for their excellent support of work at sea. We thank G. Wendt, J. Wunderlich (INNOMAR), J. Gutt, I. Vöge (AWI), F. Wenzhöfer, M. Viehweger, V. Beier, T. Wilkop, I. Busse (MPI), N. Nowald (MARUM) as well as R. Usbeck, W. Dimmler, S. Gauger (FIELAX) for technical support and laboratory work, and A. Judd for important information on seep structures of the North Sea.

References

Amann, R. I., Krumholz, L., and Stahl, D. A.: Fluorescent-oligonucleotide probing of whole cells for determinative, phylogenetic, and environmental studies in microbiology, J. Bacteriol., 172(2), 762–770, 1990.

Biddle, J. F., Lipp, J. S., Lever, M. A., Lloyd, K. G., Sørensen, K. B., Anderson, R., Fredricks, H. F., Elvert, M., Kelly, T. J., Schrag, D. P., Sogin, M. L., Brenchley, J. E., Teske, A., House, C. H., and Hinrichs, K. U.: Heterotrophic Archaea dominate sedimentary subsurface ecosystems off Peru, Proc. Natl. Acad. Sci., 103(10), 3846–3851, 2006.

Blumenberg, M., Seifert, R., Reitner, J., Pape, T., and Michaelis, W.: Membrane lipid patterns typify distinct anaerobic methanotrophic consortia, Proc. Natl. Acad. Sci., 101(30), 11 111–11 116, 2004.

Boetius, A. Ravenschlag, K., Schubert, C. J., Rickert, D. Widdel, F., Gieseke, A., Amann, R., Jørgensen, B. B., Witte, U., and Pfannkuche, O.: A marine microbial consortium apparently mediating anaerobic oxidation of methane, Nature, 407, 623–626, 2000.

Daims, H., Bruhl, A., Amann, R., Schleifer, K. H., and Wagner, M.: The domain-specific probe EUB338 is insufficient for the detection of all Bacteria: Development and evaluation of a more comprehensive probe set, Syst. Appl. Microbiol., 22(3), 434–444, 1999.

Dando, P. R., Bussmann, I., Niven, S. J., O'Hara, S. C. M, Schmaljohann, R., and Taylor, L. J.: A methane seep area in the Skagerrak, the habitat of the pogonophore *Siboglinum poseidoni* and the bivalve mollusc *Thyasira sarsi*, Mar. Ecol. Prog. Ser., 107, 157–167, 1994.

Eisma, D. and Kalf, J.: Dispersal, concentration and deposition of suspended matter in the North Sea, J. Geol. Soc. London., 144, 161–178, 1987.

Elvert, M., Boetius, A., Knittel, K., and Jørgensen, B. B.: Characterization of Specific Mem-

brane Fatty Acids as Chemotaxonomic Markers for Sulfate-Reducing Bacteria Involved in Anaerobic Oxidation of Methane, Geomicrobiol. J., 20(4), 403–419, 2003.
Fang, J., Shizuka, A., Kato, C., and Schouten, S.: Microbial diversity of cold-seep sediments in Sagami Bay, Japan, as determined by 16S rRNA gene and lipid analyses, FEMS Microbiol. Ecol., 57(3), 429–441, 2005.
Hinrichs, K.-U., Hayes, J. M., Silva, S. P., Brewer, P. G., and DeLong, E. F.: Methane-consuming archaebacteria in marine sediments, Nature, 398, 802–805, 1999.
Hinrichs, K.-U. and Boetius, A.: The Anaerobic Oxidation of Methane: New Insights in Microbial Ecology and Biogeochemistry, in: Ocean Margin Systems, edited by: Wefer, G., Billett, D., and Hebbeln, D., Springer-Verlag, Berlin Heidelberg, 457–477, 2002.
Hovland, M.: On the self-sealing nature of marine seeps, Cont. Shelf. Res., 22(16), 2387–2394, 2002.
Hovland, M.: Discovery of prolific natural methane seeps at Gullfaks, northern North Sea, Geo-Mar. Lett., 27(2), 197–201, 2007.
Hovland, M., Gardner, J. V., and Judd, A. G.: The significance of pockmarks to understanding fluid flow processes and geohazards, Geofluids, 2(2), 127–136, 2002.
Hovland, M. and Judd, A. G.: Seabed pockmarks and seepages. Graham and Trotham, London, 293 pp., 1988.
Hovland, M., Judd, A. G., Burke Jr., R. A.: The global flux of methane from shallow submarine sediments, Chemosphere, 26(1–4), 559–578, 1993.
Hovland, M. and Risk, M.: Do Norwegian deep-water coral reefs rely on seeping fluids? Mar. Geol., 198(1–2), 83–96, 2003.
Hovland, M. and Sommerville, J.H.: Characteristics of two natural gas seepages in the North Sea, Mar. Petrol. Geol., 4(2), 319–326, 1985.
Inagaki, F., Kuypers, M. M. M., Tsunogai, U., Ishibashi, J., Nakamura, K. Treude, T., Ohkubo, S., Nakaseama, M., Gena, K., Chiba, H., Hirayama, H., Nunoura, T., Takai, K., Jorgensen, B. B., Horikoshi, K., and Boetius, A.: Microbial community in a sediment-hosted CO_2 lake of the southern Okinawa Trough hydrothermal system, Proc. Natl. Acad. Sci., 103(38), 14 164–14 169, 2006.
Ishii, K., Mussmann, M., MacGregor, B. J., and Amann, R.: An improved fluorescence in situ hybridization protocol for the identification of bacteria and archaea in marine sediments, FEMS Microbiol. Ecol., 50(3), 203–212, 2004
Jørgensen, B. B. and Fenchel, T.: The sulfur cycle of a marine sediment model system, Mar.

Biol., 24(3), 189–201., 1974.
Joye, S. B., Boetius, A., Orcutt, B. N., Montoya, J. P., Schulz, H. N., Erickson, M. J., and Lugo S.: The anaerobic oxidation of methane and sulfate reduction in sediments from Gulf of Mexico cold seeps, Chemical Geology 205, 219–238, 2004.
Judd, A. G.: A global importance and context of methane escape from the seabed, Geo-Mar. Lett., 23, 147–154, 2003.
Judd, A. and Hovland, M.: Seabed Fluid Flow: The Impact on Geology, Biology and the Marine Environment, Cambridge University Press, 492 pp., 2007.
Kallmeyer, J., Ferdelman, T. G., Weber, A., Fossing, H., and Jorgensen, B. B.: A cold chromium distillation procedure for radiolabeled sulfide applied to sulfate reduction measurements, Limnol. Oceanogr. Meth., 2, 171–180, 2004.
Kane, M. D., Poulsen, L. K., and Stahl, D. A.: Monitoring the enrichment and isolation of sulfate-reducing bacteria by using oligonucleotide hybridization probes designed from environmentally derived 16S rRNA sequences, Appl. Env. Microbiol., 59, 682–686, 1993.
Knittel, K., Boetius, A., Lemke, A., Eilers, H., Lochte, K., Pfannkuche, O., Linke, P., and Amann, R.: Activity, distribution, and diversity of sulfate reducers and other bacteria in sediments above gas hydrate (Cascadia margin, Oregon), Geomicrobiol. J., 20(4), 269–294, 2003.
Knittel, K., Lösekann, T., Boetius, A., Kort, R., and Amann, R.: Diversity and Distribution of Methanotrophic Archaea at Cold Seeps, Appl. Environ. Microbiol., 71, 467–479, 2005.
Lane, D. J., Pace, B., Olsen, G. J., Stahl, D. A., Sogin, M. L., and Pace, N. R.: Rapid Determination of 16S Ribosomal RNA Sequences for Phylogenetic Analyses, Proc. Natl. Acad. Sci., 82(20), 6955–6959, 1985.
Levin, L. A.: Ecology of cold seep sediments: Interactions of fauna with flow, chemistry and microbes, in: ceanography and Marine Biology: An Annual Review., edited by: Gibson, R. N., Atkinson, R. J. A., Gordon, J. D. M., Taylor & Francis, London, UK, 1–46, 2005.
Llobet-Brossa, E., Rossello-Mora, R., and Amann, R.: Microbial Community Composition of Wadden Sea Sediments as Revealed by Fluorescence In Situ Hybridization, Appl. Environ. Microbiol., 64(7) 2691–2696, 1998.
Lösekann, T., Knittel, K., Nadalig, T., Fuchs, B. Niemann, H., Boetius, A., and Amann, R.: Diversity and Abundance of Aerobic and Anaerobic Methane Oxidizers at the Haakon Mosby Mud Volcano, Barents Sea. Appl. Environ. Microbiol., 73(10), 3348–3362, 2007.
Ludwig, W. Strunk, O., Westram, R., Richter, L., Meier, H., Yadhukumar, Buchner, A., Lai, T., Steppi, S., Jobb, G., Forster, W., Brettske, I., Gerber, S., Ginhart, A. W., Gross, O., Grumann,

S., Hermann, S., Jost, R., Konig, A., Liss, T., Lussmann, R., May, M., Nonhoff, B., Reichel, B., Strehlow, R., Stamatakis, A., Stuckmann, N., Vilbig, A., Lenke, M., Ludwig, T., Bode, A., and Schleifer, K.-H.: ARB: a software environment for sequence data, Nucl. Acids Res., 32(4), 1363–1371, 2004.

Luff, R. and Wallmann, K.: Fluid flow, methane fluxes, carbonate precipitation and biogeochemical turnover in gas hydrate-bearing sediments at Hydrate Ridge, Cascadia Margin: Numerical modeling and mass balances, Geochim. Cosmochim. Ac., 67(18), 3403–3421, 2003.

Manz, W., Eisenbrecher, M., Neu, T. R., and Szewzyk, U.: Abundance and spatial organization of Gram-negative sulfate-reducing bacteria in activated sludge investigated by in situ probing with specific 16 S rRNA targeted oligonucleotides, FEMS Microbiol. Ecol., 25, 43–61, 1998.

Massana, R., Murray, A., Preston, C., and DeLong, E.: Vertical distribution and phylogenetic characterization of marine planktonic Archaea in the Santa Barbara Channel, Appl. Environ. Microbiol., 63, 50–56, 1997.

Meyer-Reil, L.-A.: Benthic response to sedimentation events during autumn to spring at a shallow water station in the Western Kiel Bight, Mar. Biol., 77(3), 247–256, 1983.

Mills, H. J., Hodges, C., Wilson, K., MacDonald, I. R., and Sobecky, P. A.: Microbial diversity in sediments associated with surface-breaching gas hydrate mounds in the Gulf of Mexico, FEMS Microbiol. Ecol., 46, 39–52, 2003.

Mills, H. J., Martinez, R. J., Story, S., and Sobecky, P. A.: Characterization of Microbial Community Structure in Gulf of Mexico Gas Hydrates: Comparative Analysis of DNA- and RNA-Derived Clone Libraries, Appl. Environ. Microb., 71(6), 3235–3247, 2005.

Moss, C. W. and Lambert-Fair, M. A.: Location of double bonds in monounsaturated fatty acids of Campylobacter cryaerophila with dimethyl disulfide derivatives and combined gas chromatography-mass spectrometry, J. Clin. Microbiol., 27(7), 1467–1470, 1989.

Muyzer, G., Teske, A., Wirsen, C. O., and Jannasch, H. W.: Phylogenetic relationships of *Thiomicrospira* species and their identification in deep-sea hydrothermal vent samples by denaturing gradient gel electrophoresis of 16S rDNA fragments, Arch. Microbiol., 164(3), 165–172, 1995.

Nauhaus, K., Boetius, A., Krüger, M., and Widdel, F.: In vitro demonstration of anaerobic oxidation of methane coupled to sulphate reduction in sediments from a marine gas hydrate area, Environ. Microbiol., 4(5), 296–305, 2002.

Nauhaus, K., Albrecht, M., Elvert, M., Boetius, A., and Widdel, F.: In vitro cell growth of marine

archaeal-bacterial consortia during anaerobic oxidation of methane with sulfate, Environ. Microbiol., 9, 187–196, 2007.
Nelson, D. C. and Jannasch, H. W.: Chemoautotrophic growth of a marine Beggiatoa in sulfide-gradient cultures, Arch. Microbiol., 136(4), 262–269, 1983.
Nelson, D. C., Jorgensen, B. B., and Revsbech, N. P.:. Growth pattern and yield of a chemoautotrophic Beggiatoa sp. in oxygen-sulfide microgradients, Appl. Environ. Microb., 52(2), 225–233, 1986.
Nelson, D. C., Wirsen, C. O., and Jannasch, H. W.: Characterization of Large, Autotrophic Beggiatoa spp. Abundant at Hydrothermal Vents of the Guaymas Basin, Appl. Environ. Microbiol., 55(11), 2909–2917, 1989.
Niemann, H. and Elvert, M.: Diagnostic lipid biomarker and stable carbon isotope signatures of microbial communities mediating the anaerobic oxidation of methane with sulphate, Chem. Geol., in press.
Niemann, H., Elvert, M., Hovland, M., Orcutt, B., Judd, A., Suck, I., Gutt, J., Joye, S., Damm, E., K. Finster, K., and Boetius, A.: Methane emission and consumption at a North Sea gas seep (Tommeliten area), Biogeosciences, 2(4) 335–351, 2005.
Niemann, H., Lösekann, T., de Beer, D., Elvert, M., Nadalig, T., Knittel, K., Amann, R., Sauter, E. J., Schlüter, M., Klages, M., Foucher, J. P., and Boetius, A.: Novel microbial communities of the Haakon Mosby mud volcano and their role as a methane sink, Nature, 443(7113), 854–858, 2006.
Orphan, V. J., Hinrichs, K.-U., Ussler, W., Paull, C. K., Taylor, L. T., Sylva, S. P., Hayes, J. M. and Delong, E. F.: Comparative Analysis of Methane-Oxidizing Archaea and Sulfate-Reducing Bacteria in Anoxic Marine Sediments, Appl. Environ. Microbiol, 67(4), 1922–1934, 2001a.
Orphan, V. J., House, C. H., Hinrichs, K.-U., McKeegan, K. D., and DeLong, E. F.: Methane-Consuming Archaea Revealed by Directly Coupled Isotopic and Phylogenetic Analysis, Science, 293(5529), 484–487, 2001b.
Orphan, V. J., House, C. H., Hinrichs, K.-U., McKeegan, K. D., and DeLong, E. F.: Multiple archaeal groups mediate methane oxidation in anoxic cold seep sediments, Proc. Natl. Acad. Sci., 99(11), 7663–7668, 2002.
Pernthaler, A., Pernthaler, J., and Amann, R.: Fluorescence In Situ Hybridization and Catalyzed Reporter Deposition for the Identification of Marine Bacteria, Appl Environ. Microbiol., 68(6), 3094–3101, 2002.

Ravenschlag, K., Sahm, K., Pernthaler, J., and Amann, R.: High bacterial diversity in permanently cold marine sediments, Appl. Environ. Microb., 65(9), 3982–3989, 1999.
Reeburgh, W.: Oceanic methane biogeochemistry, Chem. Rev., 107(2): 486–513, 2007.
Rehder, G., Keir, R. S., Suess, E., and Pohlmann, T.: The Multiple Sources and Patterns of Methane in North Sea Waters, Aquat. Geochem., 4(3), 403–427, 1998.
Rise, L., Saettem, J., Fanavoll, S., Thorsnes, T., Ottesen, D., and Boe, R.: Sea-bed pockmarks related to fluid migration from Mesozoic bedrock strata in the Skagerrak offshore Norway, Mar. Petrol. Geol., 16(7), 619–631, 1999.
Ritger, S., Carson, B., and Suess, E.: Methane-derived authigenic carbonates formed by subduction-induced pore-water expulsion along the Oregon/ Washington margin, Geol. Soc. Am. Bull., 98(2), 147–156, 1987.
Rohmer, M., Bouvier-Nave, P., and Ourisson, G.: Distribution of hopanoid triterpenes in prokaryotes, Microbiology, 30(55), 1137–1150, 1984.
Rusch, A., Forster, S., and Huettel, M.: Bacteria, diatoms and detritus in an intertidal sandflat subject to advective transport across the water-sediment interface, Biogeochemistry, 55, 1–27, 2001.
Rusch, A., Huettel, M., Reimers, C. E., Taghon, G. L., and Fuller, C. M.: Activity and distribution of bacterial populations in Middle Atlantic Bight shelf sands, FEMS Microbiol. Ecol., 44, 89–100, 2003.
Stahl, D. A. and Amann, R.: Development and application of nucleic acid probes, in: Nucleic Acid Techniques in Bacterial Systematics, edited by: Stackebrandt, E. and Goodfellow, M., John Wiley & Sons Ltd., Chichester, UK, 205–248, 1991.
Teske, A., Hinrichs, K. U., Edgcomb, V., de Vera Gomez, A., Kysela, D., Sylva, S. P., Sogin, M. L., and Jannasch, H. W.: Microbial diversity of hydrothermal sediments in the Guaymas Basin: Evidence for anaerobic methanotrophic communities, Appl. Environ. Microb., 68(4), 1994–2007, 2002.
Trasher, J., Fleet, A. J., Hay, S. J., Hovland, M., and Düpenbecker, S.: Understanding geology as the key to using seepage in exploration: spectrum of seepage styles, in: Hydrocarbon migration and its near-surface expression, efited by: Schumacher, D. and Abrams, M. A., AAPG Memoir, 223–241, 1996.
Treude, T., Boetius, A., Knittel, K., Nauhaus, K., Elvert, M., Krüger, M., Lösekann, T., Wallmann, K., Jorgensen, B. B., Widdel, F., and Amman, R.: Anaerobic oxidation of methane at Hydrate Ridge (OR), Geochim. Cosmochim. Ac., 67(18), 491–491, 2003.

Treude, T., Knittel, K., Blumenberg, M., Seifert, R., and Boetius, A.: Subsurface microbial methanotrophic mats in the Black Sea, Appl. Environ. Microb., 71(10), 6375–6378, 2005.
Treude, T., Krüger, M., Boetius, A., and Jørgensen, B. B.: Environmental control on anaerobic oxidation of methane in the gassy sediments of Eckernfoerde Bay(German Baltic), Limnol. Oceanogr. 50(6), 1771–1786, 2005.
Valentine, D. L. and Reeburgh, W. S.: New perspectives on anaerobic methane oxidation, Environ. Microbiol., 2(5), 477–487, 2000.
Widdel, F. and Bak, F.: Gram-negative mesophilic sulfate-reducing bacteria, in: The prokaryotes, Balows, T. H., Dworkin, A., Harder, M., and Schleifer, W., Springer, Berlin Heidelberg New York, 3352–3378, 1992.
Widdel, F., Musat, F., Knittel, K., and Galushko, A.: Anaerobic degradation of hydrocarbons with sulphate as electron acceptor, in: Sulphate-reducing bacteria: environmental and engineered systems, Barton, L. L. and Hamilton, W. A., Cambridge University Press, Cambridge, UK, 265–304, 2007.
Wieringa, E. B. A., Overmann, J., and Cypionka, H.: Detection of abundant sulphate-reducing bacteria in marine oxic sediment layers by a combined cultivation and molecular approach, Environ. Microbiol., 2(4), 417–427, 2000.
Zhang, C. L. Huang, Z., Cantu, J., Pancost, R. D., Brigmon, R. L., Lyons, T. W., and Sassen, R.: Lipid Biomarkers and Carbon Isotope Signatures of a Microbial (Beggiatoa) Mat Associated with Gas Hydrates in the Gulf of Mexico, Appl. Environ. Microbiol., 71(4), 2106–2112, 2005.

Table 1. Visited gas escape structures and the presence of gas flares and methane-derived carbonates. The cruises took place in June 2002 (HE169), October 2002 (HE180), May 2004 (HE208), and September 2005 L (AL267) n.a.–bottom observations were not available, #described in Judd and Hovland 2007.

Structure	Latitude	Longitude	Water depth	Cruise	gas escape	authigenic carbonates
Gullfaks seep	61°10.40′	02°14.50′	150 m	HE 169, HE 180, AI 267, HE 208	yes	no
Holene Trench	59°19.60′	01°57.60′	130–145 m	HE 169	no	yes#
UK 15/25 pockmarks	58°17.00′	00°58.50′	155–170 m	HE 180, HE 208	yes	yes
Witch's Hole	57°56.50′	00°23.30′	135 m	HE 208	no	yes#
Snow White's Hole	57°58.81′	00°23.30′	145 m	HE 208	yes	n.a.
Tommeliten	56°29.90′	02°59.80′	75 m	HE 169, HE 180, AL 267	yes	yes
Skagerrak pockmarks	58°00.00′	09°40.00′	120–150 m	HE 208	no	no#

Table 2. Biomarker concentrations and their isotopic signatures in sediments from bacterial mat covered sands (Gullfaks Station 766), and sediments (Tommeliten Station 1274-K3) as well as from the subsurface SMTZ of Tommeliten (155 cm data by Niemann et al., 2005).n.d.=not detected; n.a.=not available.

	Gullfaks Station 766(0–10 cm)		Tommeliten 1274-K3(0–10 cm)		Tommeliten Core 1904155 cm SMTZ	
Compound	μg gdw^{-1}	δ^{13}C VPDB	μg gdw^{-1}	δ^{13}C VPDB	μg gdw^{-1}	δ^{13}C VPDB
$C_{14:0}$	1.27	−60	0.64	−30	0.15	−28
i-$C_{15:0}$	0.61	−41	0.30	−35	0.06	−43
ai-$C_{15:0}$	0.64	−42	0.43	−34	0.14	−43
$C_{15:0}$	0.40	−48	0.22	−38	0.07	−37
$C_{16:1\omega7c}$	24.04	−59	2.54	−38	0.02	−38
$C_{16:1\omega5c}$	3.79	−77	0.39	−51	0.01	n.a.
$C_{16:0}$	6.17	−46	1.93	−32	0.60	−31
10Me-$C_{16:0}$	0.45	−39	0.21	−33	0.02	n.a.
i-$C_{17:0}$	0.12	n.d.	0.06	−39	0.04	n.a.
ai-$C_{17:0}$	0.09	n.d.	0.07	−37	0.04	n.a.
cy-$C_{17:0}$	0.24	−40	0.27	−59	n.a.	n.a.
$C_{17:0}$	0.16	−36	0.08	−29	0.04	n.a.
isoprenFA-$C_{19:0}$	0.38	−34	0.13	−27	n.a.	n.a.
$C_{18:1\omega9c}$	0.91	−37	0.65	−26	0.27	n.a.
$C_{18:1\omega7c}$	6.65	−41	1.60	−45	0.06	−32
$C_{18:0}$	0.35	−37	0.32	−30	0.35	−34
Diplopterol	0.43	−84	n.d.	n.d.	n.a.	n.a.
archaeol	0.05	−115	0.05	−86	0.47	−61
sn2-hydro.arch	0.16	−117	0.31	−90	0.08	−80

CC BY

Table 3. Overview of bacterial and archaeal 16 S rRNA gene libraries and number of clones retrieved for the individual phylogenetic groups. Gullfaks (HE208, MUC766, 0–10 cm); Tommeliten (Bacterial patch 4–6 cm, AL267 1274 K3-2) and Tommeliten deep SMTZ sulfate methane transition zone (HE 180 1904, 160 cm, Niemann et al., 2005).

		Gullfaks	Tommeliten (bact. patch)	Tommeliten (deep SMTZ)
Bacteria				
Alphaproteobacteria		1	1	
Gammaproteobacteria	Methylomonas	4		
	Methylophaga	2		
	Rel. of sulfur-oxidizing symbionts	15		
	Thioalkalivibrio, Thioploca rel.		18	
	Oceanospirillales		1	
Deltaproteobacteria	Seep-SRB1	1	3	51
	Seep-SRB2			3
	Seep-SRB3	3		
	Seep-SRB4	1		
	Desulfobacterium anilini rel.	4	3	4
	Desulfobacterium rel.		1	2
	Desulfobulbus rel.	1	29	
	Myxobacteriales rel.		12	
	Desulfuromonas rel.	1		
Epsilonproteobacteria		3	2	
Spirochaeta			1	
Cytophaga/Flavobacterium/Bacteriodetes		19	4	3
Planctomycetales			3	4
Verrucomicrobia	Victivalliaceae	3	1	36
Nitrospira			1	6
Holophaga/Acidobacterium		4	10	
Nitrospina		2		
OP11		1		
Actinobacteria		2	7	
Firmicutes	Desulfotomaculum rel.	3	1	
Thermomicrobia			4	
Cyanobacteria			1	
unaffiliated		4	5	3
	Total bacterial clones analyzed	69	107	117
Archaea				
Euryarchaeota	ANME-1		17	16
	ANME-2a	63		
	ANME-2c		83	
–	Marine Benthic Group D	1		1
–	Methanococcoides		1	
Crenarchaeota	Marine Benthic Group B	3	1	
	Marine Group 1	2		
	Total archaeal clones analyzed	69	102	17

CC BY

Table 4. In situ quantification of different microbial groups using CARD-FISH. The specific probes used for CARD-FISH are listed in Materials and Methods. n.a., not analyzed; * present, but not countable.

Depth (cm)	Total single cell counts (TCC) (10^9 cm^{-1})	Bacteria (single cells)		Archaea			(single cells)		Aggregates		
		Bacteria % of TCC	DSS % TCC	Archaea % TCC	ANME-1- % TCC	ANME-2a- % TCC	ANME-2c- % TCC	ANME-3- % TCC	ANME-2a-aggregates (10^6 cm^{-3})	ANME-2c-aggregates (10^6 cm^{-3})	ANME-3-aggregates (10^6 cm^{-3})
Gullfaks 766											
0–10	7.9	46	8	12	<0.1	2	2	0	5.6	8.4	n.a.
10–20	3.0	37	12	10	<0.1	1	2	0	4.8	4.8	n.a.
20–30	0.85	39	7	n.a.	0.5	0	<1	0	0	0	n.a.
Gullfaks 771											
0–10	6.7	50	18	8	<0.1	<1	<1	0	6.6	0.4	n.a.
10–20	3.6	26	29	8	<0.1	0.9	<0.5	0	0.8	0.4	n.a.
20–30	1.3	29	31	16	<0.1	0	0	0	0.6	0	n.a.
Tommeliten 1274-K1											
0–3	4	69	25	10	<1	<1	2	<0.5	1.0	0	0
Tommeliten 1274-K2											
0–3	7	74	20	4	1	2	2	1	1.1	0	0
Tommeliten 1274-K3											
0–3	6	71	28	13	2	1	0	1	1.6	0	*
3–6	4	80	28	7	n.a.	<0.1	0	5	2.7	0	*
6–10	3	91	34	4	4	<0.1	0	2	0.9	0	*

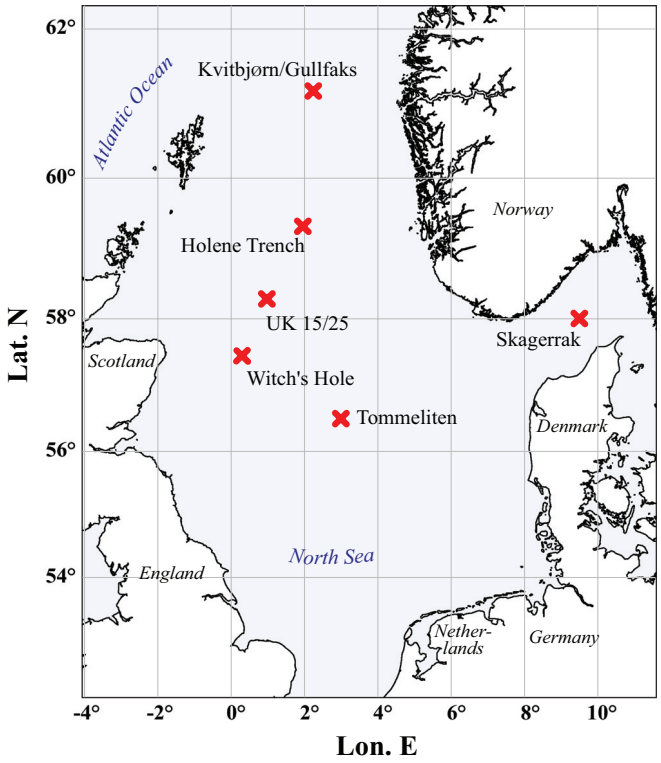

Fig. 1. Tommeliten, Gullfaks and other potential gas escape structures investigated for current gas emission during the METROL research expeditions HE 169, HE 180, HE 208 and Alkor 267.

BGD
5, 971–1015, 2008

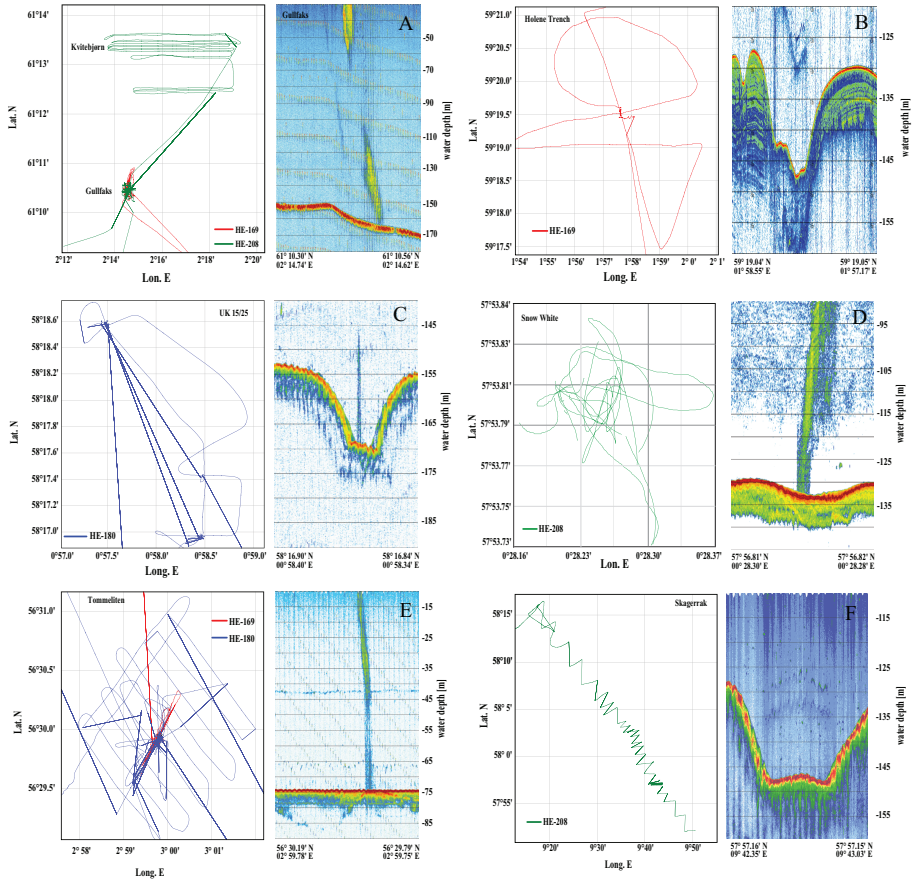

Fig. 2. Survey tracks and exemplary SES-2000 echo images showing gas flares and sea floor structures of the sites Gullfaks with the 'Heincke' seep area **(A)**, Holene Trench **(B)**, Scanner pockmark (UK 15/25 field) **(C)**, Snow White's Hole **(D)**, Tommeliten **(E)** and Skagerrak **(F)**.

BGD
5, 971–1015, 2008

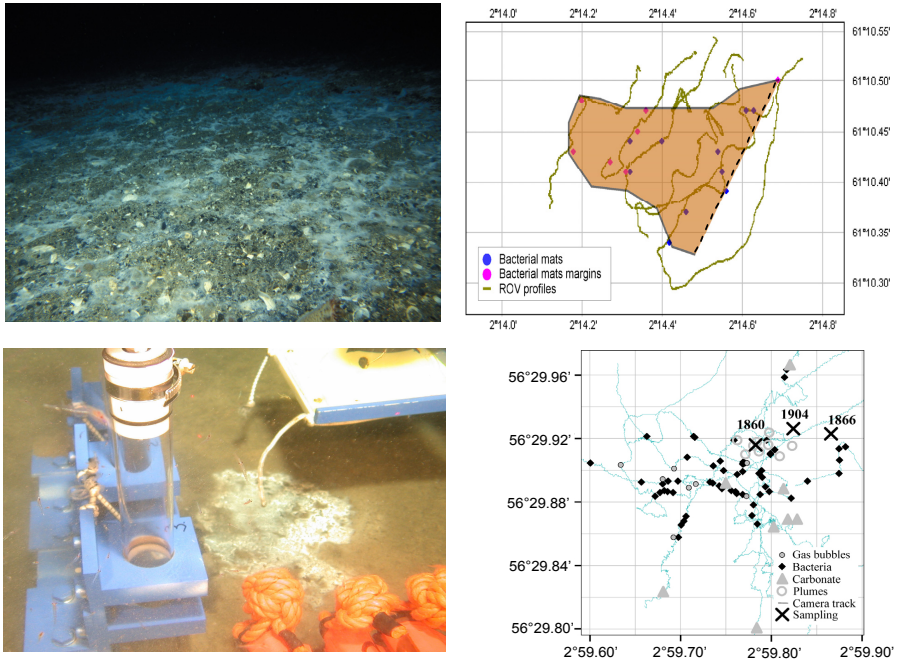

Fig. 3. **(A)** Mats of giant sulfide-oxidizing bacteria covering coarse sands and pebbles at the Heincke seep area at Gullfaks (left panel). The mats coincide with the area of gas ebullition and cover an area of about 0.1 km^2 (right panel). **(B)** Bacterial mats of the Tommeliten gas seep. Left panel: Sampling of a mat patch with a diameter of about 30 cm. Gas ebullition was observed during sampling. Right panel: Map showing the distribution of mats, gas flares and carbonates (after Niemann et al., 2005).

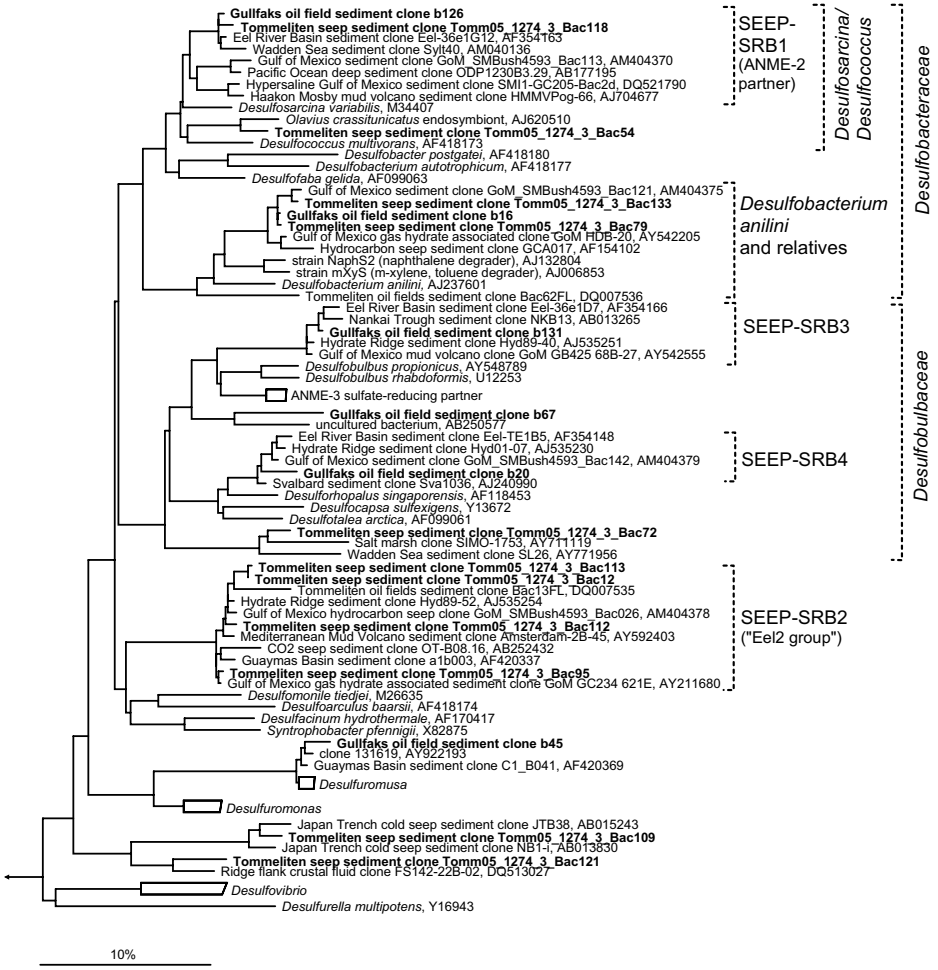
Gullfaks oil field sediment clone b126
Tommeliten seep sediment clone Tomm05_1274_3_Bac118
Eel River Basin sediment clone Eel-36e1G12, AF354163
Wadden Sea sediment clone Sylt40, AM040136
Gulf of Mexico sediment clone GoM_SMBush4593_Bac113, AM404370
Pacific Ocean deep sediment clone ODP1230B3.29, AB177195
Hypersaline Gulf of Mexico sediment clone SMI1-GC205-Bac2d, DQ521790
Haakon Mosby mud volcano sediment clone HMMVPog-66, AJ704677
Desulfosarcina variabilis, M34407
Olavius crassitunicatus endosymbiont, AJ620510
Tommeliten seep sediment clone Tomm05_1274_3_Bac54
Desulfococcus multivorans, AF418173
Desulfobacter postgatei, AF418180
Desulfobacterium autotrophicum, AF418177
Desulfofaba gelida, AF099063
Gulf of Mexico sediment clone GoM_SMBush4593_Bac121, AM404375
Tommeliten seep sediment clone Tomm05_1274_3_Bac133
Gullfaks oil field sediment clone b16
Tommeliten seep sediment clone Tomm05_1274_3_Bac79
Gulf of Mexico gas hydrate associated clone GoM HDB-20, AY542205
Hydrocarbon seep sediment clone GCA017, AF154102
strain NaphS2 (naphthalene degrader), AJ132804
strain mXyS (m-xylene, toluene degrader), AJ006853
Desulfobacterium anilini, AJ237601
Tommeliten oil fields sediment clone Bac62FL, DQ007536
Eel River Basin sediment clone Eel-36e1D7, AF354166
Nankai Trough sediment clone NKB13, AB013265
Gullfaks oil field sediment clone b131
Hydrate Ridge sediment clone Hyd89-40, AJ535251
Gulf of Mexico mud volcano clone GoM GB425 68B-27, AY542555
Desulfobulbus propionicus, AY548789
Desulfobulbus rhabdoformis, U12253
ANME-3 sulfate-reducing partner
Gullfaks oil field sediment clone b67
uncultured bacterium, AB250577
Eel River Basin sediment clone Eel-TE1B5, AF354148
Hydrate Ridge sediment clone Hyd01-07, AJ535230
Gulf of Mexico sediment clone GoM_SMBush4593_Bac142, AM404379
Gullfaks oil field sediment clone b20
Svalbard sediment clone Sva1036, AJ240990
Desulforhopalus singaporensis, AF118453
Desulfocapsa sulfexigens, Y13672
Desulfotalea arctica, AF099061
Tommeliten seep sediment clone Tomm05_1274_3_Bac72
Salt marsh clone SIMO-1753, AY711119
Wadden Sea sediment clone SL26, AY771956
Tommeliten seep sediment clone Tomm05_1274_3_Bac113
Tommeliten seep sediment clone Tomm05_1274_3_Bac12
Tommeliten oil fields sediment clone Bac13FL, DQ007535
Hydrate Ridge sediment clone Hyd89-52, AJ535254
Gulf of Mexico hydrocarbon seep clone GoM_SMBush4593_Bac026, AM404378
Tommeliten seep sediment clone Tomm05_1274_3_Bac112
Mediterranean Mud Volcano sediment clone Amsterdam-2B-45, AY592403
CO2 seep sediment clone OT-B08.16, AB252432
Guaymas Basin sediment clone a1b003, AF420337
Tommeliten seep sediment clone Tomm05_1274_3_Bac95
Gulf of Mexico gas hydrate associated sediment clone GoM GC234 621E, AY211680
Desulfomonile tiedjei, M26635
Desulfoarculus baarsi, AF418174
Desulfacinum hydrothermale, AF170417
Syntrophobacter pfennigii, X82875
Gullfaks oil field sediment clone b45
clone 131619, AY922193
Guaymas Basin sediment clone C1_B041, AF420369
Desulfuromusa
Desulfuromonas
Japan Trench cold seep sediment clone JTB38, AB015243
Tommeliten seep sediment clone Tomm05_1274_3_Bac109
Japan Trench cold seep sediment clone NB1-i, AB013830
Tommeliten seep sediment clone Tomm05_1274_3_Bac121
Ridge flank crustal fluid clone FS142-22B-02, DQ513027
Desulfovibrio
Desulfurella multipotens, Y16943
10%
SEEP-SRB1 (ANME-2 partner)
Desulfosarcina/ Desulfococcus
Desulfobacteraceae
Desulfobacterium anilini and relatives
SEEP-SRB3
Desulfobulbaceae
SEEP-SRB4
SEEP-SRB2 ("Eel2 group")

Fig. 4.

Fig. 4. Phylogenetic tree showing the affiliations of bacterial 16S rRNA clone sequences from Gullfaks and Tommeliten to selected references of the Deltaproteobacteria. The tree was calculated on a subset of nearly full length sequences by maximum-likelihood analysis in combination with filters, which considered only 50% conserved regions of the 16S rRNA of δ-proteobacteria to exclude the influence of highly variable positions. Partial sequences were inserted into the reconstructed tree by using parsimony criteria with global-local optimization, without allowing changes in the overall tree topology. Probe specificity is indicated by brackets. The bar represents 10% estimated sequence divergence. Sequences from this study are written in bold.

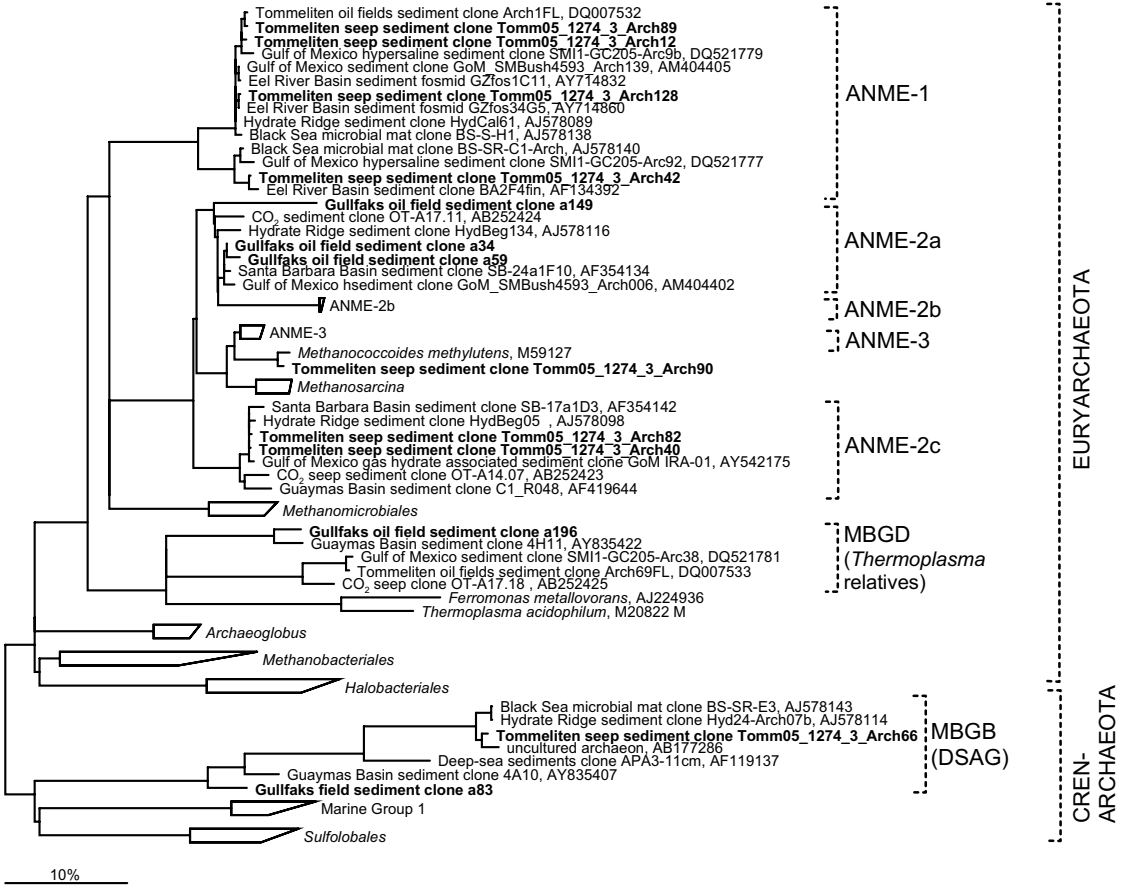
Tommeliten oil fields sediment clone Arch1FL, DQ007532
Tommeliten seep sediment clone Tomm05_1274_3_Arch89
Tommeliten seep sediment clone Tomm05_1274_3_Arch12
Gulf of Mexico hypersaline sediment clone SMI1-GC205-Arc9b, DQ521779
Gulf of Mexico sediment clone GoM_SMBush4593_Arch139, AM404405
Eel River Basin sediment fosmid GZfos1C11, AY714832
Tommeliten seep sediment clone Tomm05_1274_3_Arch128
Eel River Basin sediment fosmid GZfos34G5, AY714860
Hydrate Ridge sediment clone HydCal61, AJ578089
Black Sea microbial mat clone BS-S-H1, AJ578138
Black Sea microbial mat clone BS-SR-C1-Arch, AJ578140
Gulf of Mexico hypersaline sediment clone SMI1-GC205-Arc92, DQ521777
Tommeliten seep sediment clone Tomm05_1274_3_Arch42
Eel River Basin sediment clone BA2F4fin, AF134392
Gullfaks oil field sediment clone a149
CO2 sediment clone OT-A17.11, AB252424
Hydrate Ridge sediment clone HydBeg134, AJ578116
Gullfaks oil field sediment clone a34
Gullfaks oil field sediment clone a59
Santa Barbara Basin sediment clone SB-24a1F10, AF354134
Gulf of Mexico hsediment clone GoM_SMBush4593_Arch006, AM404402
ANME-2b
ANME-3
Methanococcoides methylutens, M59127
Tommeliten seep sediment clone Tomm05_1274_3_Arch90
Methanosarcina
Santa Barbara Basin sediment clone SB-17a1D3, AF354142
Hydrate Ridge sediment clone HydBeg05 , AJ578098
Tommeliten seep sediment clone Tomm05_1274_3_Arch82
Tommeliten seep sediment clone Tomm05_1274_3_Arch40
Gulf of Mexico gas hydrate associated sediment clone GoM IRA-01, AY542175
CO2 seep sediment clone OT-A14.07, AB252423
Guaymas Basin sediment clone C1_R048, AF419644
Methanomicrobiales
Gullfaks oil field sediment clone a196
Guaymas Basin sediment clone 4H11, AY835422
Gulf of Mexico sediment clone SMI1-GC205-Arc38, DQ521781
Tommeliten oil fields sediment clone Arch69FL, DQ007533
CO2 seep clone OT-A17.18 , AB252425
Ferromonas metallovorans, AJ224936
Thermoplasma acidophilum, M20822 M
Archaeoglobus
Methanobacteriales
Halobacteriales
Black Sea microbial mat clone BS-SR-E3, AJ578143
Hydrate Ridge sediment clone Hyd24-Arch07b, AJ578114
Tommeliten seep sediment clone Tomm05_1274_3_Arch66
uncultured archaeon, AB177286
Deep-sea sediments clone APA3-11cm, AF119137
Guaymas Basin sediment clone 4A10, AY835407
Gullfaks field sediment clone a83
Marine Group 1
Sulfolobales
10%
ANME-1
ANME-2a
ANME-2b
ANME-3
ANME-2c
MBGD
(Thermoplasma
relatives)
MBGB
(DSAG)
EURYARCHAEOTA
CREN-
ARCHAEOTA

Fig. 5.

Fig. 5. Phylogenetic tree showing the affiliations of archaeal 16S rRNA gene sequences retrieved from sediments underlying the microbial mats of Gullfaks and Tommeliten to selected references of the domain Archaea. Besides cultivated organisms, at least one representative per phylogenetic group of all previously published clone sequences from methane-rich sites is included as references. The tree was constructed by using maximum-likelihood analysis in combination with filters excluding highly variable positions. Partial sequences were inserted into the reconstructed tree by using parsimony criteria with global-local optimization, without allowing changes in the overall tree topology. Probe specificity is indicated by brackets. The bar represents 10% estimated sequence divergence. Sequences from this study are written in bold.

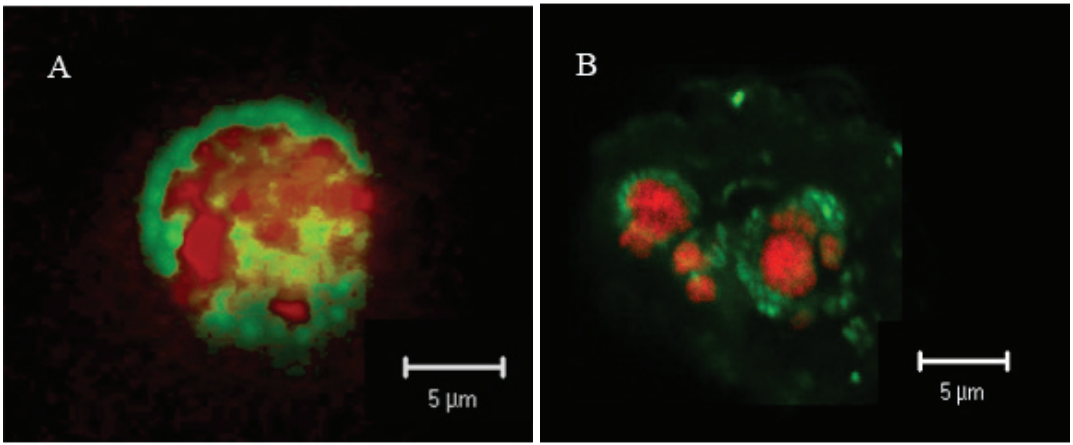

Fig. 6. Dual hybridizations with fluorescently labeled rRNA targeting oligonucleotide probes. **(A)** Consortia of ANME 2a/DSS from Gullfaks (probes ANME2a-647 [red] and DSS658 [green]); **(B)** Consortia of ANME2c/DSS from Tommeliten (probes ANME2c-622 [red] and DSS-658 [green]).